

CHARACTERIZATION OF LOIRE RIVER SAND IN THE SMALL STRAIN DOMAIN USING NEW BENDER-EXTENDER ELEMENTS

Christophe Dano¹
Hocine Hareb²
Pierre-Yves Hicher¹

ABSTRACT

New piezo-ceramics transducers called bender-extender elements are used to characterize the mechanical behavior of the alluvial Loire River sand in the small strain domain. An unique couple of bender-extender elements is necessary to transmit and/or receive both compression waves and shear waves. Therefore, the simultaneous identification of the Young's modulus E_{\max} and the shear modulus G_{\max} in the small strain domain is possible along isotropic and deviatoric stress paths.

Keywords: Young's modulus, shear modulus, Loire River sand

BENDER-EXTENDER ELEMENTS

Since their appearance at the end of the 70's (Shirley & Hampton, 1978), bender elements have become an usual geotechnical testing device. Bender elements are piezo-ceramics transducers which could be embedded into different laboratory apparatus such as triaxial cells (see for instance Dyvik & Madhus, 1986 ; Brignoli *et al.*, 1996 ; Kuwano *et al.*, 1999 ; Lo Presti *et al.*, 1999 ; Dano & Hicher, 2002), oedometer cells (Dyvik & Olsen, 1989)... These transducers transmit and receive shear waves (also noted S-waves). The wave propagation causes very small strains ($\varepsilon \leq 0.001$ %) and enables the determination of the shear modulus G_{\max} in the small strain domain (Viggiani & Atkinson, 1995 ; Dano & Hicher, 2002). A review of the bender elements technique can be found in the paper by Brignoli *et al.* (1996).

Independent compression waves transducers (P-waves) were sometimes associated with bender elements in order to identify another parameter of the Hooke's law, either the Young's modulus E_{\max} or the Poisson's ratio ν (Brignoli *et al.*, 1996).

However, the simultaneous use of compression wave transducers and shear wave transducers has not been extensively developed until now. In order to remedy this inconvenience, Lings & Greening (2001) described a new transducer called bender-extender element. An unique couple of such bender-extender elements can transmit and receive both P-waves and S-waves : this property results from a slight modification of bender elements.. Therefore, these elements can be

¹ Civil Engineering Laboratory of Nantes Saint-Nazaire, Member of the Research Institute in Civil and Mechanical Engineering, Ecole Centrale Nantes, BP 92101, 44321 NANTES (France). E-mail: Christophe.Dano@ec-nantes.fr

² Formerly Master of Science at the Civil Engineering Laboratory of Nantes Saint-Nazaire

used to easily identify the Young's modulus E_{\max} and the shear modulus G_{\max} in the small strain domain simultaneously : in this paper, they are tested on a Loire River sand as presented later on.

This simplicity also holds true in respect of the acquisition data system. The device requires a personal computer and a control box as shown in Fig. 1. Likewise, the sample preparation is hardly changed by the introduction of the bender-extender elements embedded into the lower and upper pedestals of a conventional triaxial cell.

The principle of bender-extender elements is straightforward. The transmitter is excited by an electric signal : the new user-friendly system allows the experimenter to choose between a square signal, a sinusoidal signal or an user-defined signal. The input signal induces longitudinal (for P-waves) or tangential vibrations (for S-waves) which are propagated through the sample. The receiver is then submitted to longitudinal or tangential displacements which are inversely converted into an output electric signal. The input and output electric signals are recorded on the PC for a subsequent analysis. It has to be noted that the displacement amplitude in extension is about one order of magnitude smaller than the bending displacement (Lings & Greening, 2001). This can explain the fact that the P-waves output signals are sometimes more difficult to interpret than the S-waves output signals.

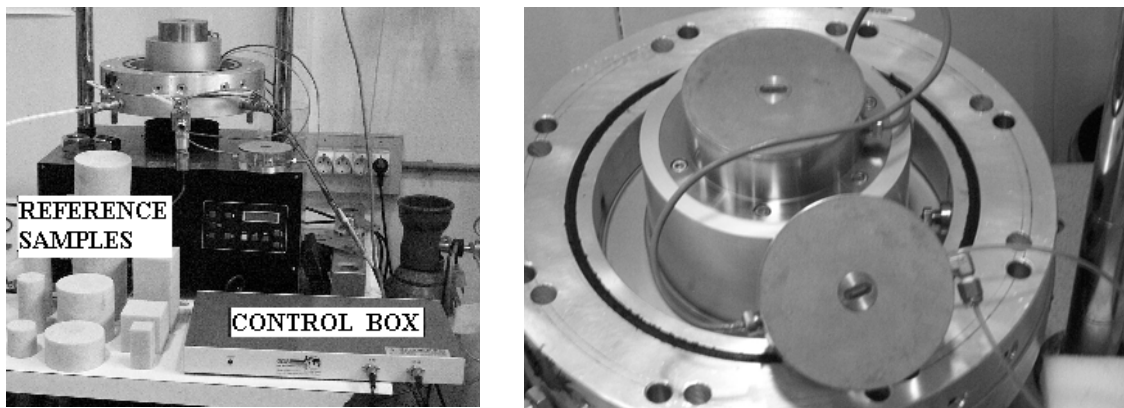


FIG. 1. Bender-Extender elements into the triaxial cell.

PHYSICAL PROPERTIES OF LOIRE RIVER SAND

The Loire River sand consists of recent alluvial deposits of the Loire River, close to its mouth in the west part of France. It is composed of sub-rounded particles and elongated shell fragments. The grading curves obtained on two samples are represented in Fig. 2. The mean grain size D_{50} is 520 μm . The coefficient of uniformity C_u is equal to 3.5. The coefficient of curvature C_c is equal to 0.8. Therefore, the Loire River sand is a poorly graded sand (ASTM D2487-93).

The specific weight γ_s of the Loire River sand grains is 26.2 kN/m^3 (ASTM D854-92). The minimum unit weight γ_{\min} (ASTM D4254-91) and the maximum unit weight γ_{\max} (ASTM D4253-93) are respectively equal to 15.1 kN/m^3 ($e_{\max} = 0.738$) and 18.5 kN/m^3 ($e_{\min} = 0.415$).

LARGE STRAIN BEHAVIOR OF LOIRE RIVER SAND

A first series of drained triaxial tests on saturated samples of Loire River sand (100 mm in diameter, 200 mm in height) was carried out, following the French Standard P 94-074. The sand

was deposited by five successive layers. Each of them was compacted by tamping. The dry unit weight was then close to 17.5 kN/m^3 . The saturation phase led to B-values greater than 0.95. Samples were consolidated under an effective mean stress between 100 and 400 kN/m^2 . They were finally sheared at a constant shear rate equal to $1.67 \times 10^{-5} \text{ s}^{-1}$.

The shortening of the sample was measured on an external gauge whereas the axial load was determined by an internal load cell. Volume changes were measured in a burette.

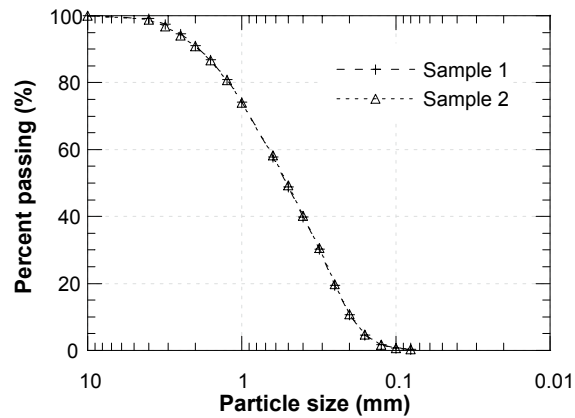


FIG. 2. Grading curves of the Loire sand.

Experimental results are presented in Fig. 3. Each test is doubled. The behavior of the Loire River sand is typical of a dense sand. The values of the parameters of the linear elastic perfectly plastic model assuming a Mohr-Coulomb yield criterion, namely :

- the tangent modulus E at the origin of the deviator stress q - axial strain ε_1 curve, measured for an axial strain equal to 0.1 % ;
- the Poisson's ratio ν at the origin of the volumetric strain ε_v - axial strain ε_1 curve ;
- the angle of dilation ψ determined at the maximum volumetric strain rate in the dilating stage ;
- the angle of friction ϕ'_p at the peak stress and the angle of friction ϕ'_{res} in the residual state determined in the Mohr-Coulomb diagram;
- the cohesion c' determined in the Mohr-Coulomb diagram

are reported in Table 1 where e_0 is the initial void ratio.

SMALL STRAIN BEHAVIOR OF LOIRE RIVER SAND

As previously stated by many authors (Iwasaki & Tatsuoka, 1977 ; Hicher, 1996), the tangent modulus E greatly underestimates the value of the Young's modulus because of the inaccuracy of conventional triaxial tests (Scholey *et al.*, 1995). In the small strain domain ($\varepsilon \leq 0.001 \%$), it is well-known that the Young's modulus E_{max} and the shear modulus G_{max} follow power laws such as (Hardin & Richart, 1963 ; Iwasaki & Tatsuoka, 1977 ; Hicher, 1996) :

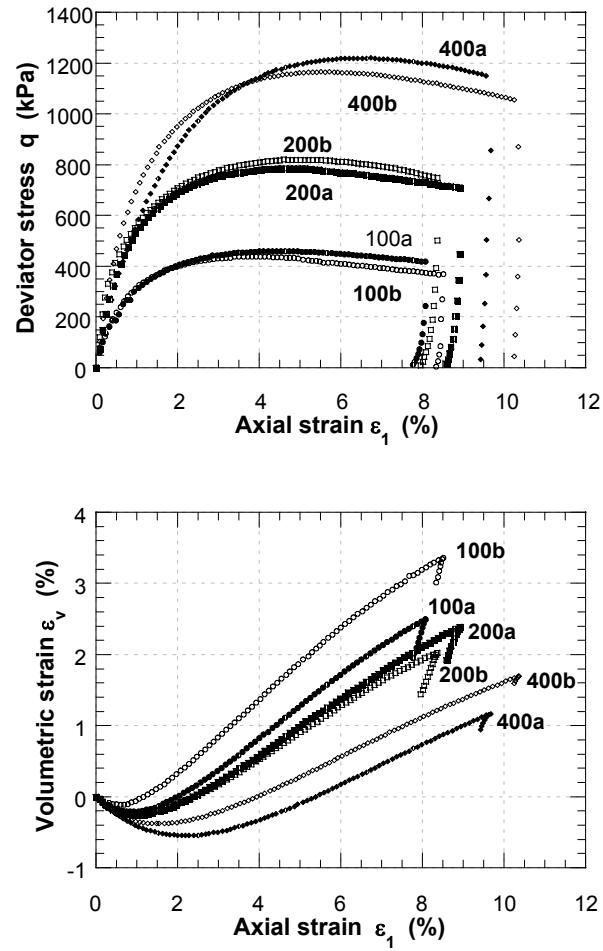


FIG. 3. Large strain triaxial tests results.

TABLE 1. Parameters of the elastic perfectly plastic model.

| Test reference | σ'_c kN/m^2 | e_0 | E MN/m^2 | ν | ψ <i>degrees</i> | c' kN/m^2 | ϕ'_p <i>degrees</i> | ϕ'_{res} <i>degrees</i> |
|----------------|-------------------------|-------|-----------------|-------|--------------------------|------------------|-----------------------------|---------------------------------|
| 100a | 100 | 0.51 | 93 | 0.22 | 10.7 | 0 | 39.2 | 33.9 |
| 100b | 100 | 0.48 | 97 | 0.27 | 12.4 | | | |
| 200a | 200 | 0.52 | 126 | 0.25 | 9.3 | | | |
| 200b | 200 | 0.48 | 118 | 0.23 | 8.9 | | | |
| 400a | 400 | 0.49 | 140 | 0.24 | 7.2 | | | |
| 400b | 400 | 0.50 | 146 | 0.21 | 6.9 | | | |

$$E_{\max} = \frac{k_E}{e} \times p'^{n_E} \quad (1)$$

$$G_{\max} = \frac{k_G}{e} \times p'^{n_G} \quad (2)$$

where e is the void ratio ; p' is the mean effective stress (in kN/m^2) ; k_E , k_G , n_E and n_G are constant values experimentally determined. If E_{\max} and G_{\max} are expressed in MN/m^2 , then k_E is between 10 and 25 and k_G is usually between 4 and 10 (Hardin & Richart, 1963 ; Iwasaki & Tatsuoka, 1977 ; Hicher, 1996 ; Dano & Hicher, 2002). The coefficients n_E and n_G are close to 0.5. Wave propagation tests on the Loire River sand were performed in order to establish similar equations for the Young's modulus $E_{v,\max}$ and the shear modulus $G_{vh,\max}$ where the subscript "v" means that the wave are vertically propagated and the subscript "h" means that the shear wave is horizontally polarized (Kuwano *et al.*, 1999).

Small strain experiments were carried out on a dry Loire River Sand in order to obtain a clear output signal for the P-waves (greatly affected by the aqueous phase). The sand was deposited by five successive layers. Each of them was compacted by tamping. The dry unit weight was then close to 17.5 kN/m^3 . A vacuum of 30 kN/m^2 was applied to the specimen during set-up within the cell. The vacuum was released and the specimen opened to the atmosphere during the application of a cell pressure σ'_c of 50 kN/m^2 . Volume changes are determined by means of the external displacement gauge and the pressure-volume controller used to apply the cell pressure in return for some corrections due to the load cell movement.

The sample was subjected to the following loading program :

- an isotropic compression stress path from 50 kN/m^2 to 400 kN/m^2 ;
- an isotropic unloading from 400 kN/m^2 to 100 kN/m^2 ;
- an isotropic compression stress path from 100 kN/m^2 to 500 kN/m^2 ;
- an isotropic unloading from 500 kN/m^2 to 200 kN/m^2 ;
- a shearing stress path at a constant cell pressure $\sigma'_c = 200 \text{ kN/m}^2$ with a shear rate of $1.67 \times 10^{-5} \text{ s}^{-1}$ until $\varepsilon_1 = 3.8 \%$;
- a discharge to an isotropic stress state with a mean effective stress $p' = 200 \text{ kN/m}^2$;
- an isotropic compression stress path from 200 kN/m^2 to 500 kN/m^2 .

Bender-extender elements were excited by sinusoidal input signals with a frequency of 5 kHz and an amplitude of 10 V. Typical signals obtained on the Loire River sand are shown in Fig. 4. Brignoli *et al.* (1996) and Jovicic *et al.* (1996) have put forward that the ratio $R_d = L / \lambda_w$ (where L is the distance of propagation of the wave and λ_w the wave length) controls the shape of the S-wave output signal. Here the ratio R_d is close to 3. This implies that near-field effects have to be taken into account for the determination of the propagation time T_s of the shear wave (Brignoli *et al.*, 1996 ; Jovicic *et al.*, 1996) : the arrival of the shear wave on the receiver corresponds to the first sign change of the signal derivative, as indicated in Fig. 4. As for the P-wave, the determination of the propagation time T_p is straightforward : the first deviation of the output signal coincides with its arrival on the receiver (Fig. 4). The respective velocities V_p and V_s of the P-wave and the S-wave are therefore calculated (Viggiani & Atkinson, 1995 ; Brignoli *et al.*, 1996 ; Jovicic *et al.*, 1996):

$$V_P = \frac{L}{T_P} \quad (3)$$

$$V_S = \frac{L}{T_S} \quad (4)$$

where L is the distance of propagation between the tips of the transducers.

Finally, the following equations are used to calculate the parameters of the Hooke's law :

$$E_{v,\max} = \rho V_S^2 \times \frac{3V_P^2 - 4V_S^2}{V_P^2 - V_S^2} \quad (5)$$

$$G_{vh,\max} = \rho V_S^2 \quad (6)$$

$$\nu = \frac{1}{2} \times \frac{V_P^2 - 2V_S^2}{V_P^2 - V_S^2} \quad (7)$$

where ρ is the density of the Loire River sand.

Along isotropic loading or unloading stress paths, the Young's modulus $E_{v,\max}$ and the shear modulus $G_{vh,\max}$ evolves as indicated in Fig. 5. The following equations are deduced from the experimental results :

- before shearing

$$E_{v,\max} \times e = 24.7 \times p'^{0.42} \quad (8)$$

$$G_{vh,\max} \times e = 9.8 \times p'^{0.42} \quad (9)$$

- after shearing

$$E_{v,\max} \times e = 20.4 \times p'^{0.45} \quad (10)$$

$$G_{vh,\max} \times e = 7.7 \times p'^{0.45} \quad (11)$$

These equations prove the fabric change caused by the shearing phase. However, what is notable is the common value of the powers n_E and n_G in the equations (8) and (9) and in the equations (10) and (11). It means that the Poisson's ratio does not change along isotropic stress paths. If $n_E = n_G$, then :

$$\nu = \frac{E}{2G} - 1 = \frac{k_E}{2k_G} - 1 \quad (12)$$

Equation (12) applied to the tests on the Loire River sand leads to a value of the Poisson's ratio ν equal to 0.26 before shearing and equal to 0.32 after shearing. This result is in accordance with the numerical results obtained by Aubry *et al.* (1982) who consider that the value of the Poisson's ratio ν does not depend on the mean effective stress p' if p' is greater than 150 kN/m².

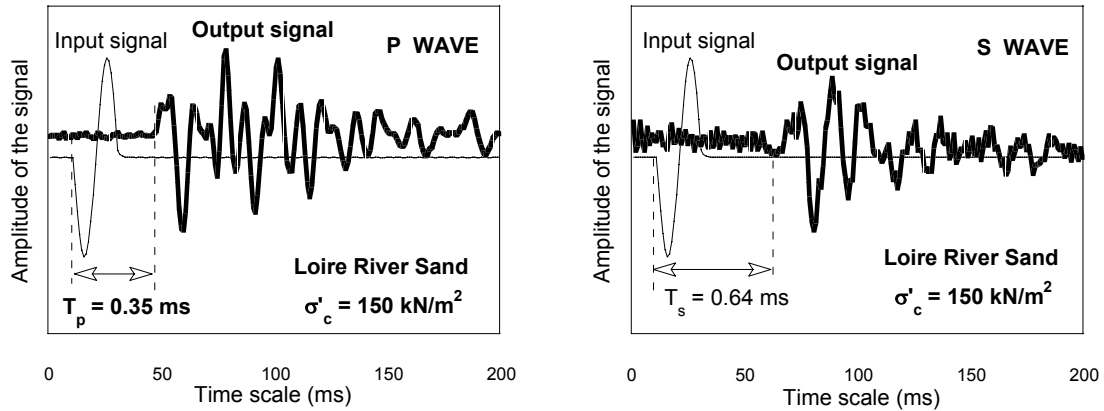


FIG. 4. Electric signals obtained by use of bender-extender elements.

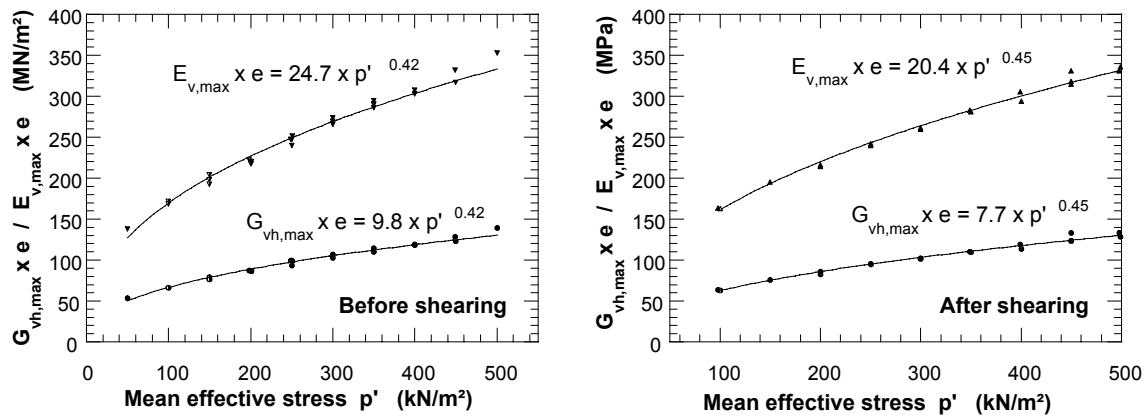


FIG. 5. Evolution of $E_{v,max}$ and $G_{vh,max}$ along isotropic stress paths (symbols : experimental data ; continuous lines : fitting curves).

CONCLUSIONS

Improved piezo-ceramics transducers have been set up within a conventional triaxial cell in order to study the mechanical behavior of the Loire River sand in the small strain domain ($\epsilon \leq 0.001\%$). An unique couple of bender-extender elements enables to transmit and receive both shear waves and compression waves. Therefore, the Young's modulus E_{max} and the shear modulus G_{max} can be simultaneously determined along isotropic and / or deviatoric stress paths.

This new device was tested on the Loire River sand. Typical laws for the Young's modulus and the shear modulus were found.

ACKNOWLEDGMENTS

The authors would like to acknowledge the companies RATP, INTRAFOR (France) for their financial support and the company GDS Instruments for their efforts in the development of the bender-extender elements.

REFERENCES

- Aubry, D., Biarez, J., Boelle, J-L. and Meunier J. (1982), "Identification of elastic coefficients through resonant tests of soils samples", Soil Dynamics & Earthquake Engineering Conference, Southampton, 65-75
- Brignoli, E.G.M., M. Gotti, and K.H. Stokoe (1996), "Measurement of shear waves in laboratory specimens by means of piezoelectric transducers", *Geotechnical Testing Journal*, **19**(4), 384–397.
- Dano, C. (2001), "Comportement mécanique des sols injectés", PhD. Thesis, Ecole Centrale of Nantes and University of Nantes (in French).
- Dano, C. and Hicher, P-Y. (2002), "Evolution of elastic shear moduli in granular materials along isotropic and deviatoric stress paths", 15th Engineering Mechanics Division Conference, New-York.
- Dyvik, R. and C. Madhus (1986), "Lab measurements of G_{max} using bender elements", Publication 161 of the Norwegian Geotechnical Institute, 1-7.
- Dyvik, R. and Olsen, T.S. (1989), " G_{max} measured in oedometer and DSS tests using bender elements", 12th International Conference on Soil Mechanics and Foundation Engineering, Rio de Janeiro, 39-42.
- Hardin, B.O. and F.E. Richart (1963), "Elastic wave velocities in granular soils", *Journal of the Geotechnical Engineering Division, ASCE*, **89**(1), 33-65.
- Hareb, H. (2002), Internal report, Civil Engineering Laboratory of Nantes Saint-Nazaire.
- Hicher, P-Y. (1996), "Elastic properties of soils", *Journal of Geotechnical Engineering*, **122**(8), 641-648.
- Iwasaki, T. and F. Tatsuoka (1977), "Effects of grain size and grading on dynamic shear moduli of sands", *Soils and Foundations*, **17**(3), 19-35.
- Jovicic, V., M.R. Coop, and M. Simic (1996), "Objective criteria for determining G_{max} from bender element tests", *Geotechnique*, **46**(2), 357-362.
- Kuwano, R., Connolly, T.M. and Kuwano, J. (1999), "Shear stiffness anisotropy measured by multi-directional bender element transducers, Proceedings of the International Symposium on Pre-failure deformation characteristics of geomaterials, Torino, Balkema, 205-212.
- Lings, M.L. and Greening, P.D. (2001), "A novel bender/extender element for soil testing", *Geotechnique*, **51**(8), 713-717.
- Lo Presti, D.C.F., Pallara, O., Jamiolkowski, M. and Cavallaro, A. (1999), "Anisotropy of small strain stiffness of undisturbed and reconstituted clays", Proceedings of the International Symposium on Pre-failure deformation characteristics of geomaterials, Torino, Balkema, 3-9.
- Scholey, G.K., J.D. Frost, D.C.F. Lo Presti, and M. Jamiolkowski (1995), "A review of instrumentation for measuring small strains during triaxial testing of soil specimens", *Geotechnical Testing Journal*, **18**(2), 137–156.
- Shirley, D.J. & Hampton, L.D. (1978), "Shear-wave measurements in laboratory sediments",

Journal of Acoustics Soc. Am., **63**(2), 607-613
Viggiani, G. and J.H. Atkinson (1995), "Interpretation of bender element tests", *Geotechnique*, **45**(1), 149–154.

Standards

ASTM D854-92. Test method for Specific gravity of soils.

ASTM D4254-91. Test methods for Minimum index density and unit weight of soils and Calculation of relative density.

ASTM D4253-93. Test methods for Maximum index density and unit weight of soils using a vibratory table.

ASTM D2487-93. Test method for Classification of soils for engineering purpose.

NF P 94-074 (1994). Essai à l'appareil triaxial – Appareillage – Préparation des éprouvettes – Essais UU – CU + u – CD.